Measuring Short Surface Waves with Stereophotography

Omar H. Shemdin and *H. Minh Tran*
Ocean Research and Engineering, 255 S. Marengo Ave., Pasadena, CA 91101

ABSTRACT: This paper discusses the implementation of close-range stereophotography to measure directional wave number spectra of short gravity waves in the ocean. Use is made of the conventional stereo-correlation technique with analytical plotters to demonstrate the use of stereophotography in this ocean application. High-pass filtering is shown to be an essential step in obtaining useful information on short surface waves that ride over the longer surface waves. Low-pass filtering is found to reduce correlation errors of short waves. The various human and machine sources of error are discussed. A wave number spectrum derived from stereophotography is compared favorably with another obtained using an *in situ* sensor, under equivalent environmental conditions.

INTRODUCTION

STEREOPHOTOGRAPHY IS A REMOTE SENSING TECHNIQUE that was developed in the early 1900s to obtain surface elevation maps of terrain [Ghosh, 1968; Wolf, 1983]. The first attempts to measure ocean surface topography using stereophotography focused on measuring long ocean waves from airborne platforms, as discussed by Cole *et al.* [1960], Sugimori [1975], and Holthuijsen [1983]. Although the stereophotography technique was found useful in obtaining the directional wave number spectrum of long waves, it has not been widely used because (1) the required data processing is labor intensive compared to conventional waveheight measuring techniques, and (2) simpler *in situ* wave measuring techniques, such as wave buoys, produce sufficiently useful information on long surface waves.

The advent of microwave remote sensing applications for the ocean has emphasized interest in short surface waves, i.e., wavelengths in the range 1 to 100 cm. Such waves are advected by the ambient current and orbital velocities of the long waves. Under such conditions, short surface waves have a Doppler frequency component imposed by the local current. The encounter frequency spectrum will not yield the intrinsic frequency spectra or an equivalent wave number spectrum, unless assumptions are made of the directional distribution of short waves. This problem is eliminated if the wave number spectrum is measured directly. A method for measuring wave number spectra using single photographs was introduced by Stillwell [1969]. The single photograph method has been used extensively by Gotwols and Irani [1980], Monaldo and Kasevich [1981], and more recently by Strizhkin *et al.* [1985]. It was found that, although the single photograph method is useful for providing wave number spectra of surface wave slopes, it is limited in its operational use by the requisite presence of uniform sky illumination. Also, the single photograph technique does not directly provide the directional wave height spectrum itself, but rather the directional slope component spectrum as measured through a $\cos^2(\theta - \theta_o)$ filter, where θ is the wave direction and θ_o is the camera look direction.

The shortcomings in available techniques for measuring short surface waves discussed above demonstrate the need for seeking improved methods. During the Tower Ocean Wave and Radar Dependence (TOWARD) experiment [Shemdin, 1988], close-range stereophotography was used as a test of concept for measuring short surface waves. The early results are discussed by Shemdin, *et al.* [1988] which focused on the geophysical aspects of short surface wave measurement. This paper focuses on the instrumental aspects, data processing techniques, error analysis, and comparison with other methods. The renewed interest in stereophotography at present is due to the availability of rapid automatic data processing that can potentially eliminate the labor intensive aspects of the stereophotography technique that had limited its use previously.

EXPERIMENTAL SET-UP AND PROCEDURE

An experiment was conducted from the Naval Oceans Systems Center (NOSC) Tower off Mission Beach, San Diego from 1984 to 1986 [Shemdin, 1988] for the purpose of demonstrating the feasibility of measuring short surface waves using stereophotography. Two synchronized Hasselblad cameras were mounted on the tower to photograph overlapping areas of the ocean. The vertical height, H, between the level of the cameras and the water surface was approximately 9.5 m (subject to tidal fluctuation). The horizontal distance, B, between the two cameras was 5.0 m. This photographic set-up results in a base to height ratio, B/H, of 0.53. The normal ratio of the eye base width, b, to the distance, h, at which the stereo model is formed is 0.15. Thus the above experiment set-up yields a vertical exaggeration factor of 3.5 $[(B/H)/(b/h)]$ compared to the human eyes. This factor allows for greater precision in measurement and is compensated for during the stereo correlation process.

The two cameras used during the TOWARD experiment were pointed in a westerly direction. The incidence angle (tilt) of each camera was set at 30°, and the azimuthal angle (convergence) was set so as to maximize the overlapping area covered by the two cameras. A horizontal T-bar was deployed from the tower at an elevation of 3.0 m above the sea surface in the view of both cameras. The T-bar was used to (1) define the area of overlap on the sea surface, and (2) provide control points for establishing the stereo processing model.

Two sets of lenses were used to obtain different areas of coverage and image resolutions. An 80-mm focal-length lens was used during TOWARD in March of 1985, and a 150-mm focal-length lens was used during the Mini TOWARD Phase of the experiment from December 1985 to January 1986. The 80-mm focal-length lens and the 150-mm focal-length lens yield 1.6-cm and 0.85-cm horizontal resolutions, respectively. The camera f-stops were set in the range from 8 to 16, and the shutter speed was set in the range from 1/1000 s to 1/250 s, depending on sky illumination. The depth of field was kept in the range of 5 to 10 m to insure continuous focus of the short waves at all phase points along the long wave profile. The selected frame rate was one per 1.5 seconds. The period of the long waves encountered off Mission Bay during the photography session was 9 seconds. Under such conditions, a series of six consecutive photographs span one long wave profile.

For rectification and stereo-correlation, the OMI Product, Model

PHOTOGRAMMETRIC ENGINEERING & REMOTE SENSING,
Vol. 58, No. 3, March 1992, pp. 311–316.

0099-1112/92/5803-311$03.00/0

ASII-AM, analytical plotter was used. A typical contoured map of the ocean surface elevations obtained using the stereo plotter is shown in Plate 1. The area of the sea surface shown in Plate 1 is 4.1 m by 4.1 m. The corresponding horizontal resolution in both the X and Y directions is 1.6 cm, and the estimated vertical resolution is 0.3 cm. In its digital form the surface is represented by an equally spaced, rectangular grid of 256 by 256 pixels. The X-axis of the map is aligned in the east-west direction.

DATA PROCESSING

The result from the stereo plotter is a 256 by 256 matrix of wave heights at equal spacings in both spatial directions. The first step in processing the data is to check the surface for discontinuous lines or spikes. This step includes visual inspection and statistical quantization. If the data file requires editing, then an average of eight surrounding points is used to interpolate a new value for each matrix element not measured. Such adjustment is rarely required during this initial step. The second step is to perform two-dimensional high-pass filtering, which removes the mean surface on which the short waves are superimposed. The mean surface masks the height and directional properties associated with the short waves. The mean surface can be simulated by least-squares fitting of surface elevations. The elevation, Z_{ij}, of a point on the mean surface can be represented by a multivariable, second-order polynomial of the form

$$Z_{ij} = a_0 + a_1 X_{ij} + a_2 Y_{ij} + a_3 X_{ij} Y_{ij} + a_4 X_{ij}^2 + a_5 Y_{ij}^2, \quad (1)$$

where a_0 through a_5 are coefficients defined by the least-squares fit. Subtracting the mean surface from the raw data yields the topography of the short surface waves. The influence of high-pass filtering is shown in Plate 2. Plate 2a shows the two-dimensional Fourier transform of the sea surface without high-pass filtering. The effect of the high-pass filter is shown in Plate 2b in the spectral domain. The comparison implies that long waves are sharply reduced by this filter.

The third step in the data processing sequence is to perform low-pass filtering of the data. The low-pass filtering step is necessary to remove the mutliplicative error in the high wave number region caused by the operator. Such low-pass filtering will be discussed in detail in the section on error analysis below.

The fourth step involves windowing the stereo images. Windows are applied to the stereo data to reduce the spectral leakage due to the discontinuities at the boundaries of the data set. A surface elevation map is a two-dimensional array of elevation

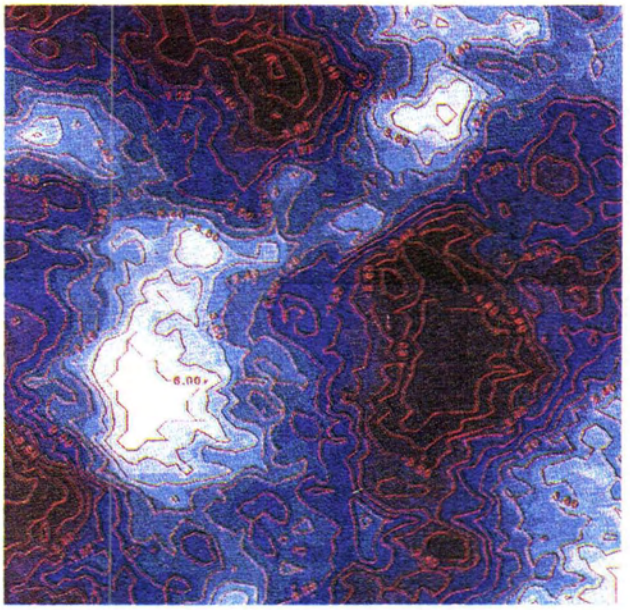

PLATE 1. Example contour map of ocean surface elevation. The surface area covered is 4.1 m by 4.1 m. The elevation contours are in cm.

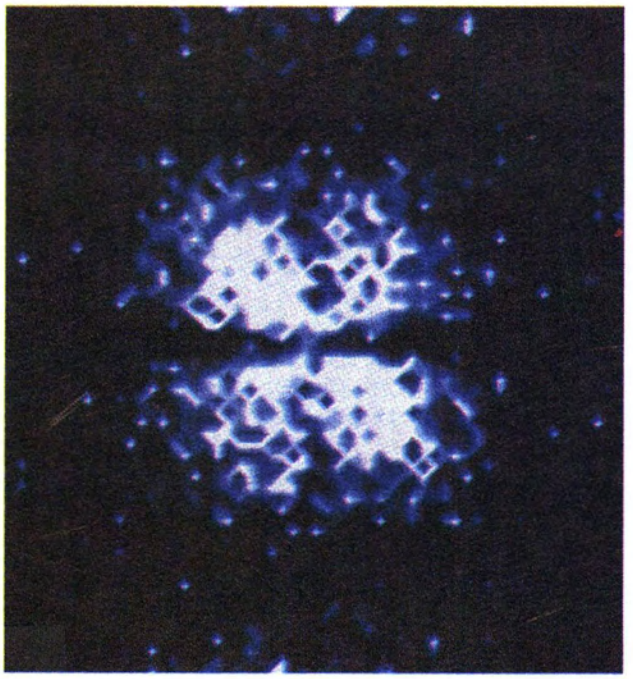

(a)

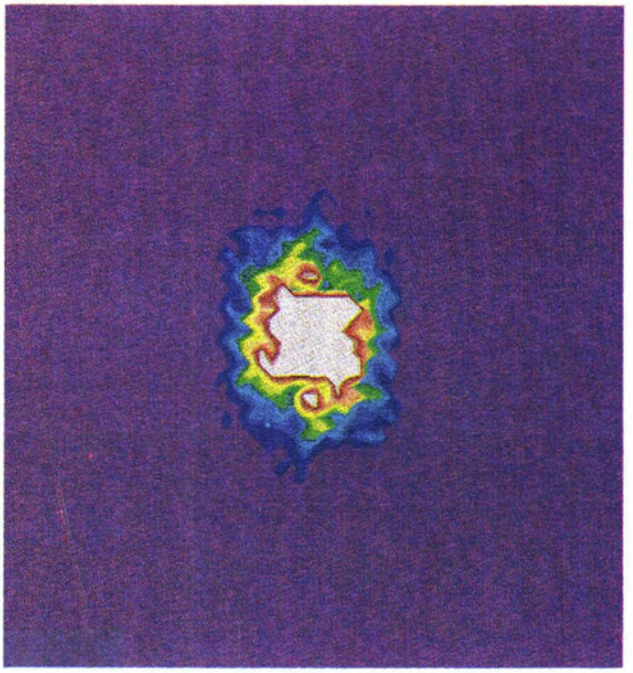

(b)

PLATE 2. (a) Two-dimensional Fourier transform of the area in Plate 1. The wave numbers are in the range 0 to 2.0 rad/cm in both directions. Color code from high to low: white, blue, purple. (b) Two-dimensional Fourier transform obtained after applying two-dimensional high-pass filter to the surface elevation in Plate 1. Color code from high to low: white, red, yellow, green, blue, purple.

values with a finite extent. This finite observation interval is not comparable to the periodic extension of a sinusoid, as would be expected in harmonic analysis. The resulting discontinuities are demonstrated in Figure 1 for one dimension. Extending to two dimensions, this step can be done by matching derivatives at the boundary or by setting these derivatives either to zero or to the proximity of zero. Thus, for a periodic extension of the data to be continuous in many orders of the derivatives, the data must be smoothly brought to zero at the boundaries.

Several well-known windows were applied to the TOWARD stereo images, and the effects on the averaged omni-directional spectra were investigated. One type of window applied is the Tukey, or cosine-tapered, window. This window is defined as

$$W(n_x, n_y) = 1.0, \ \alpha N < n_x, n_y < (1 - \alpha)N, \tag{2a}$$

$$W(n_x, n_y) = \sin\left[\frac{n_x}{\alpha N}\frac{n_y}{2}\frac{\pi}{2}\right], \ 0 < n_x, n_y \leq \alpha N, \tag{2b}$$

and

$$W(n_x, n_y) = \sin\left[\frac{n_x}{\alpha N}\frac{n_y - (1-\alpha)N}{2}\frac{\pi}{2}\right], \ (1-\alpha)N \leq n_x, n_y < N, \tag{2c}$$

where n_x, n_y are the numbers of the row or column in the array, N is the total number of rows or columns of the array, and α can be 0.1, 0.2, or 0.5 [Harris, 1978]. The different α values defined the spactial extent to which the filter is applied.

Another familiar type of window is the $\cos^\beta$ window which is defined for a finite Fourier transform as

$$W(n_x, n_y) = \sin^\beta\left[\frac{n_x}{N}\pi\right]\sin^\beta\left[\frac{n_y}{N}\pi\right], \tag{3}$$

where β is an integer from 1 through 4, with 2 being known as the Hanning window, n_x, n_y are the numbers of the row or the column in the array, and N is the total number of rows or columns of the array (the normalizing coefficient is deleted here but is discussed below).

Figure 2 shows five omni-directional spectra obtained from one identical frame, processed with five different windows. An omni-directional spectrum is obtained by directionally averaging a two-dimensional spectrum such as shown in Plate 2 (see Equations 4 to 6). Figure 2 shows that, although the different windows can have an effect on the spectral energy level, they do not significantly alter the slope of the omni-directional wave number spectrum. The filter effect on the spectral energy level is normally accounted for by incorporating a coefficient in Equations 2 or 3. The accurate measurement of this slope is important in determining the relevant dynamics in the equilibrium range associated with short surface waves.

The conversion of the two-dimensional Fourier transform of the ocean surface into an omni-directional spectrum involves converting a rectangular coordinate spectrum into a polar coordinate spectrum. For each wave number, $k = (k_x^2 + k_x^2)^{1/2}$ the spectral element area (dk_x by dk_y) is summed directionally over a ring with a width $dk(= dk_x = dk_y)$, from 0 to 2π. The portion of energy included in each ring is weighted in proportion to the area of overlap between each spectral element and the omni-directional ring. In a polar coordinate system, the omni-directional spectrum $F(k)$ is defined as

$$F(k) = \int_\theta \psi(k, \theta)d\theta, \tag{4}$$

where $\psi(k, \theta)$ is the directional wave number spectrum in a cylindrical coordinate system and θ is wave direction. The mean squared surface elevation is given by

$$<\eta^2> = \int_k F(k)kdk = \int_\theta\int_k \psi(k, \theta)kdkd\theta. \tag{5}$$

In a Cartesian coordinate system the mean squared surface elevation, $<\eta^2>$, is given by

$$<\eta^2> = \int_{-\infty}^{+\infty}\int_{-\infty}^{+\infty} \Phi(k_x, k_y)dk_xdk_y, \tag{6}$$

where $\Phi(k_x, k_y)$ is the wave nubmer spectrum in the Cartesian coordinate system.

An omni-directional spectrum may be obtained by first averaging sequential frames in the Cartesian two-dimensional Fourier domain before obtaining the omni-directional spectrum. The degrees of freedom can be increased by dividing each frame into 4 or 16 sub-blocks. The Fourier transform of each sub-block has two degrees of freedom. Hence, one frame can yield 32 degrees of freedom, and for an average of 23 sequential frames the statistical reliability reaches 736 degrees of freedom.

Dividing each frame into sub-blocks decreases the length of the longest wave that can be measured (also implied is a decrease in the wave number resolution). Figure 3 shows averaged spectra obtained by different types of frame averaging. The full size frames are shown to extend to lower wave numbers. The different spectra converge in the wave number domain greater than 0.4 rad/cm.

ERROR ANALYSIS

To validate the use of stereophotography for measuring short surface waves, it is necessary to investigate all possible sources

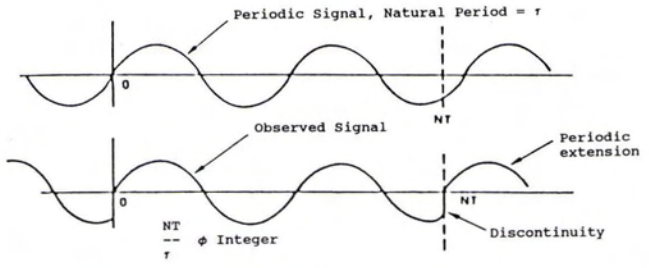

FIG. 1. Illustration of discontinuities in harmonic analysis in one dimension, (after Harris, 1978).

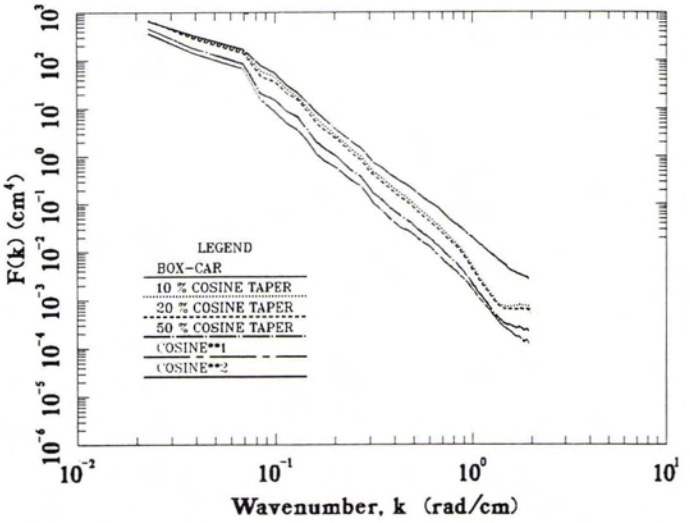

FIG. 2. Omni-directional spectra from one stereo image showing the effect of different windows.

of error associated with this method. Fifty-five pairs of stereophotographs were used to examine such errors. The frames which were considered corresponded to different meteorological conditions, horizontal and vertical resolutions, selected frames that are correlated five times independently, and selected frames that are scanned in two different directions.

An important source of error in the stereo plotter system is the uncertainty in position location. The *XY* coordinator registers each pixel with an uncertainty of 1.6 mm in the horizontal directions and 2.0 mm in the vertical direction. This error source is imposed by the precision of the coordinatograph and the truncation and round-off errors of the computer. The magnitude of this error is well within the spatial resolutions used in the TOWARD experiment (0.85 cm and 1.6 cm) and the corresponding vertical resolutions (0.3 cm and 0.6 cm, respectively) for the images processed.

Another source of error is the operator (or human) error. The stereo plotter requires the operator to view the three-dimensional image and to make judgments on perceived information such as depth, intensity, size, and texture. This type of error is random within each frame and varies from one operator to the next. Operator error cannot be determined in an absolute sense, not can it be removed easily. It is useful, however, to learn about the characteristics of operator error in the spectral domain and to compensate the computed wave number spectra prior to interpreting the results.

The first experiment aimed at this objective involved independent scans of one stereo pair by five different operators. The five independent scans were used to determine correlation coefficients between each of the four frames to the one chosen as the reference frame. The correlation coefficient is defined as

$$r = \frac{|\int <|P(K_0)Q^*(k_0)|> dk_0|^2}{\int <|P(k_0)|^2 > dk_0 \int <|Q(k_0)|^2 > dk_0}, \quad (7)$$

where $P(k_0)$ is the Fourier transform of each scanned line in the reference frame, and $Q^*(k_0)$ is the conjugate Fourier transform of the other frame. The resulting correlation coefficients are summarized in Table 1. The correlation results are interpreted to mean that the measurement of surface structure in the different frames by different operators is strongly correlated. A low correlation coefficient between the different frames would imply large errors introduced by the different operators. Hence, the results in Table 1 are indicative of relatively low operator errors in measuring surface elevation features in the stereo image.

The omni-directional spectra obtained for each of the five independently correlated frames are shown in Figure 4a. Here, the five independent correlations are by the same operator. Vis-

TABLE 1. CORRELATION COEFFICIENTS OF FIVE INDEPENDENT SCANS OF ONE STEREO-PAIR (FRAMES A1, A1, A3, A4, A5 ARE THE SURFACE ELEVATION MAPS OF A SINGLE STEREO-PAIR TAKEN ON 22 JANUARY 1986 AT 15:45:18 HOUR, WIND SPEED EQUAL TO 2 M/S).

Reference Frame	Compared Frame	Correl. Coeff.
A1	A1	1.0
A1	A2	0.91
A1	A3	0.96
A1	A4	0.96
A1	A5	0.81

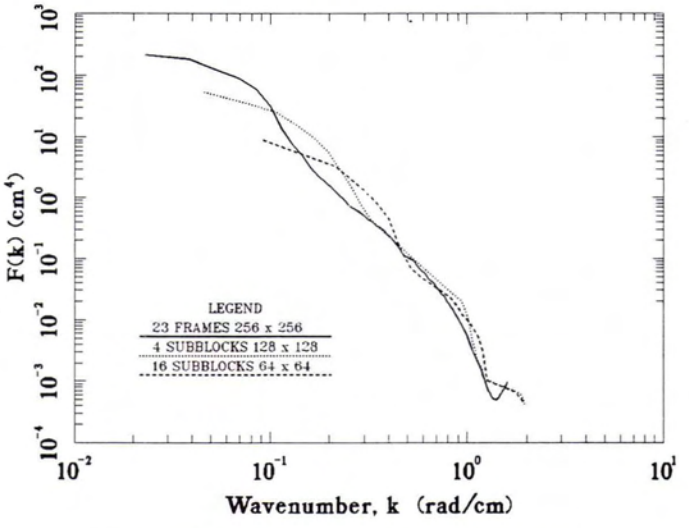

FIG. 3. Omni-directional wave number spectra average over (———) 23 Frames, (. . . . . .) four sub-blocks of one frame, and (- - - - -) 16 sub-blocks of one frame.

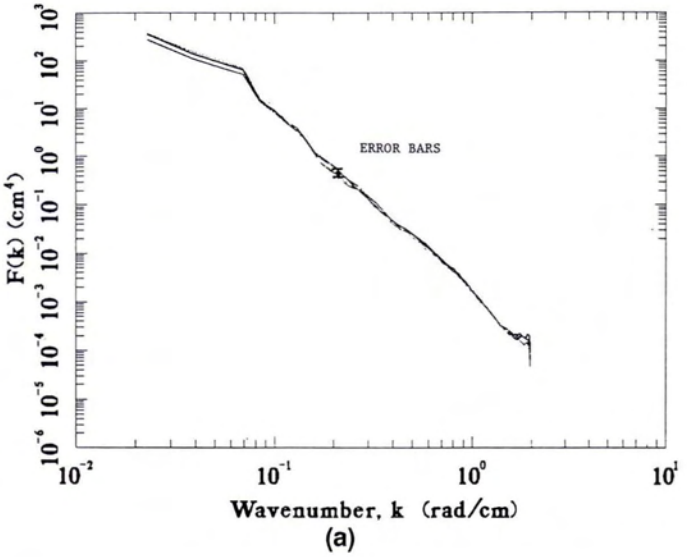

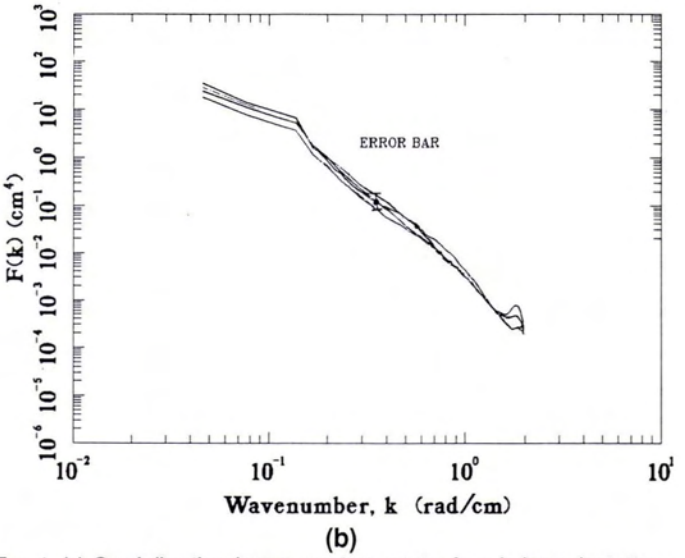

FIG. 4. (a) Omni-directional wave number spectra from independent stereo correlations of one frame by an expert stereo operator. (b) Omni-directional wave number spectra from five independent stereo correlations of the same frame in Figure 4a by five different stereo operators.

ual inspection of these spectra show good agreement. A similar result is given in Figure 4b when the independent correlations are by five different operators. The spectral characteristics of these frames remain unchanged even when the energy level is estimated to be within ±10 percent in Figure 4a and within ±22 percent in Figure 4b.

Another source of error is the accuracy of the stereo plotting instrument to continuously scan an image. The stereo plotter is designed to scan a line of x-number of elements at any one time, then move by y-increment and scan the next line. In theory, the pencil point that follows the surface should return to the exact x-position where it started, but at $(y + \Delta y)$ position. In reality this is not the case. The pencil point moves to a position that has been shifted in either or both spatial directions. The shifting distances are very small. Hence, it can only affect the spectrum in the higher wave number region. For an omni-directional spectrum this error can be clearly demonstrated by taking the average of one-dimensional Fourier Transforms of the 256 lines in the scan direction and comparing it to the average of the 256 lines scanned in the cross-scan direction. Such a comparison is shown in Figure 5. The two curves in this figure have similar slopes in wave numbers less than 0.6 rad/cm, corresponding to 10 cm in wavelength. At higher wave numbers an error deck is witnessed in the cross-scanned direction. This type of error deck appears persistently in all the frames analyzed in this study.

To remove this error and to resolve the omni-directional spectrum beyond a 10-cm wavelength, a method using low-pass filtering is used. Assuming the error to be multiplicative noise, the waveheight error is represented as

$$h_e(x + \Delta x, y + \Delta y) = h(x,y)[1 + N(x,y)], \qquad (8)$$

where N is the multiplicative noise function. Using Equation 8, this error can be reduced by taking the logarithm of the data and computing the inverse logarithm after applying a nine-point, two-dimensional running average to the data [Oppenheim and Schafer, 1975]. Figure 6 shows the averaged spectra in both the scanned and cross-scanned directions after applying the above low-pass filter. The slope of the cross-scanned-direction spectrum now levels out at about 1.5 rad/cm, or 4-cm wavelength. In Figure 7 the omni-directional wave number spectra corresponding to Figures 5 and 6 are shown. Applying the low-pass filtering technique appears to clearly lower the noise deck in the high wave number region, and allows establishment of a well defined upper slope for the wave number spectrum.

Finally, as a test of data quality of a stereo-produced omni-directional wave number spectrum, a comparison is provided in Figure 8 with an equivalent wave number spectrum derived from a laser-optical sensor mounted on a wave follower [Shemdin and Hwang, 1988]. The agreement is considered favorable, as assumptions are made in converting the time series from the slope sensor to a wave number spectrum.

SUMMARY AND CONCLUSION

The use of stereophotography for measuring short surface waves was investigated during the TOWARD experiment. Using conventional stereoplotting techniques, 55 stereo pairs were analyzed to investigate the errors generated by measurements from stereophotography. The results derived from this study suggest that high-pass filtering is essential for extracting useful information on short surface waves. Errors introduced by the stereo operator in aligning the lines being scanned imposes a

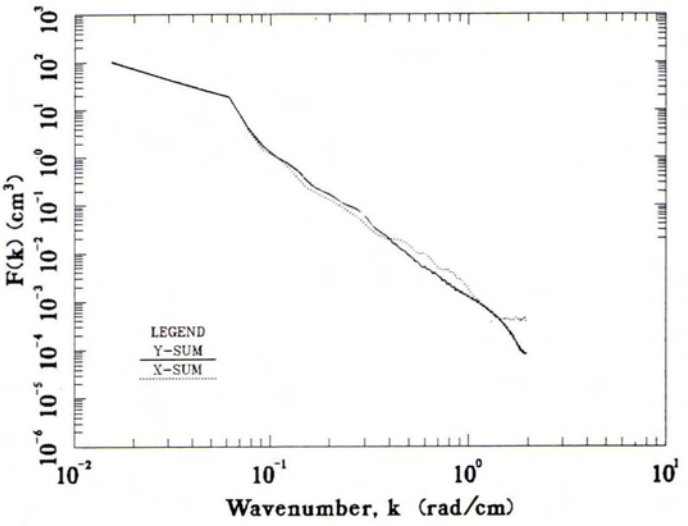

FIG. 6. Results shown in Figure 5 after removing the multiplicative noise given by Equation 8.

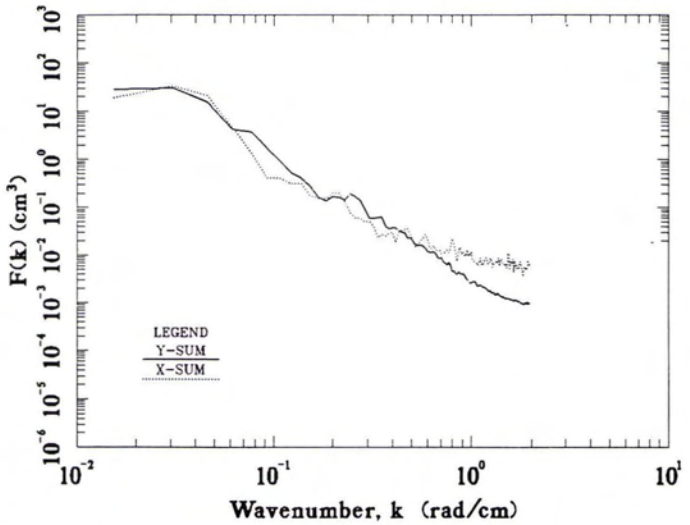

FIG. 5. Average of 256-line wave number spectra in the along-scan direction (———) and in the cross-scan direction (. . . . . .).

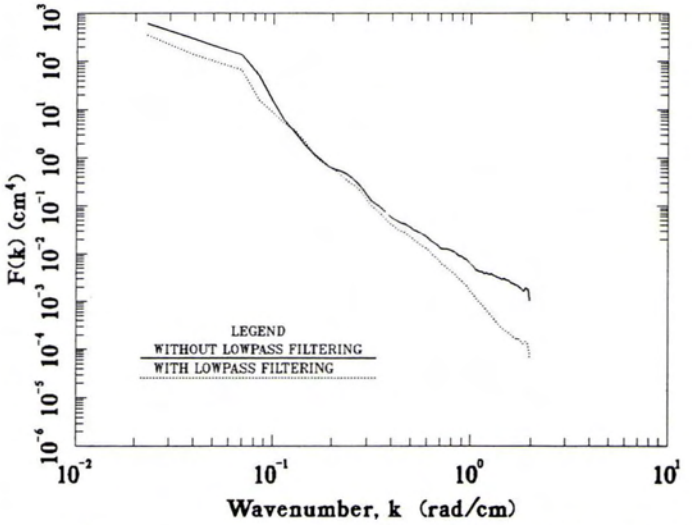

FIG. 7. Omni-directional wave number spectra before and after applying the low pass filter given by Equation 8.

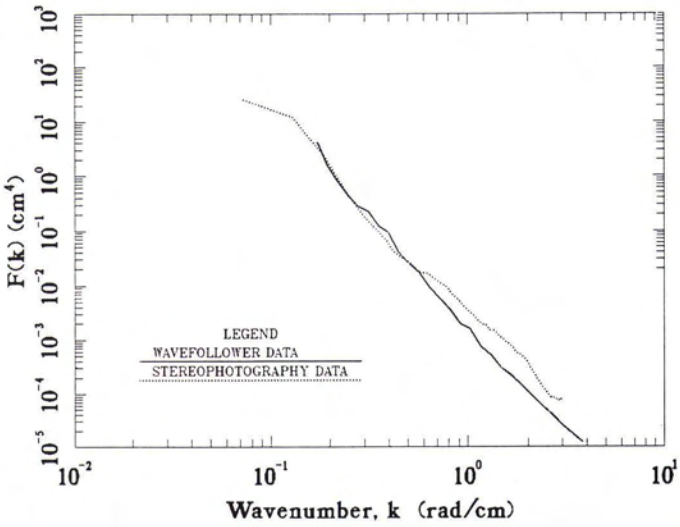

FIG. 8. Comparison of equivalent omni-directional wave number spectra obtained with stereophotograph (. . . . .) and from laser-optical data (—).

limitation on measuring waves that are shorter than 10 times the digitized resolution cell. The operator error can be reduced when low-pass filtering of the data is applied.

The wave number spectra obtained from stereophotography compare favorably with those derived from converted *in situ* slope time series. The central conclusion derived from this proof-of-concept study is that stereophotography is a highly viable technique for measuring elevations of short gravity waves, yielding wave number spectra of short waves directly. The primary disadvantage of the stereophotography technique is that it is labor intensive in the manual correlation mode. However, manual correlation can be replaced with digital data processing techniques, which are now readily available. The digital techniques allow, in addition, removal of the human and analytical stereo plotter sources of error.

ACKNOWLEDGMENTS

The stereophotographic correlation was executed by a team of operators at the U.S. Geological Survey under the supervision of S.C. Wu and F.J. Schafer. P.A. Hwang and D.P. Kasilingam of Ocean Research and Engineering provided valuable inputs in the analysis phase. W.J. Pierson, Jr., of City University of New York reviewed the results and provided helpful comments on the processing of data. The effort was sponsored by the Office of Naval Research under the SAR Research Program with H. Dolezalek as the Scientific Officer.

REFERENCES

Cote, L. F., J. O. Davis, W. Marks, R. F. McGough, E. Mehr, W. J. Pierson, Jr., J. F. Ropek, G. Stephenson, and R. C. Vetter, 1960. The Directional Spectrum of a Wind Generated Sea as Determined from Data Obtained by the Stereo Wave Observations Project, *Meteorological Papers*,Vol. 2, No. 6, New York University, 88 p.

Ghosh, S. K., 1968. *Theory of Stereophotogrammetry*, Ohio State University Dept. of Geodetic Science, Columbus Ohio.

Gotwols, B. L., and G. B. Irani, 1980. Optical Determination of the Phase Velocity of Short Gravity Waves, *J. Geophys. Res.*, 85:3964–3970.

Harris, F. J., 1978. On the Use of Windows for Harmonic Analysis with the Discrete Fourier Transform, *Proc. IEEE*, 66:51–83.

Holthuijsen, L. H., 1983. Observations of the Directional Distribution of Ocean-Wave Energy in Fetch-Limited Conditions, *J. Phys. Oceanogr.*, 13:191–207.

Monaldo, F. M., and R. S. Kasevich, 1981. Daylight Imagery of Ocean Surface Waves for Wave Spectra, *J. Phys. Oceanogr.*, 11:272–283.

Oppenheim, A. V., and R. W. Schafer, 1975. *Digital Signal Processing*, Prentice-Hall, Englewood Cliffs, New Jersey.

Shemdin, O. H., 1988. Tower Ocean Wave and Radar Dependence Experiment: An Overview, *J. Geophys. Res.*, 93:13,829–13,836.

Shemdin, O. H., and P. A. Hwang, 1988. Comparison of Measured and Predicted Sea Surface Spectra of Short Waves, *J. Geophys. Res.*, 93:13,883–13,890.

Shemdin, O. H., H. M. Tran, and S. W. Wu, 1988. Directional Measurement of Short Ocean Waves With Stereophotography, *J. Geophys. Res.*, 93:13,891–13,901.

Stillwell, D., 1969. Directional Energy of Sea Waves from Photographs, *J. Geophys. Res.*, 74:1974–1986.

Strizhkin, I. I., M. P. Lapchinskaya, Yu. A. Il'in, and V. A. Malinnikov, 1985. Spatial Structure of High-Frequency Wind Waves on the Sea for Different Meteorological Conditions, *Izv. Atmos. Oceanic Phys.*, 21:342–344.

Sugimori, Y., 1975. A Study of the Application of the Holographic Method to the Determination of the Directional Spectrum of Ocean Waves, *Deep Sea Res.*, 22:339–350.

Wolf, P. R., 1983. *Elements of Photogrammetry, 2nd Edition*, McGraw-Hill Book Company.

(Received 2 November 1990; revised and accepted 15 May 1991)